p. 78 (unpublished).
[46]Reviewed by C. T. Tomizuka, in *Methods of Experimental Physics*, edited by K. Lark-Horovitz and V. A. Johnson (Academic, New York, 1959), Vol. 6A, p. 364.
[47]R. N. Jeffery and D. Lazarus, J. Appl. Phys. 41, 3186 (1970).
[48]E. S. Fisher and D. Dever, in *The Science, Technology and Application of Titanium*, edited by R. I. Jaffee and N. E. Promisel (Pergamon, Oxford, 1970), p. 373.
[49]C. Kittel, *Introduction to Solid State Physics*, 3rd ed. (Wiley, New York, 1966), p. 183.
[50]M. W. Zemansky, *Heat and Thermodynamics*, 4th ed. (McGraw-Hill, New York, 1957), p. 251.
[51]L. R. Holland, J. Appl. Phys. 34, 2350 (1963).
[52]J. Spreadborough and J. W. Christian, Proc. Phys. Soc. (London) 74, 609 (1959).
[53]J. C. Fisher, J. Appl. Phys. 22, 74 (1951).
[54]R. T. P. Whipple, Phil. Mag. 45, 1225 (1954).
[55]H. S. Levine and C. J. MacCallum, J. Appl. Phys. 31, 595 (1960).
[56]T. Suzuoka, Trans. Japan Inst. Metals 2, 25 (1961).
[57]A. D. McQuillan and M. K. McQuillan, *Titanium* (Academic, New York, 1956), p. 409.
[58]R. W. Keyes, J. Chem. Phys. 29, 467 (1958).
[59]R. W. Keyes, in *Solids Under Pressure*, edited by W. Paul and D. M. Warschauer (McGraw-Hill, New York, 1963), p. 71.
[60]A. W. Lawson, S. A. Rice, R. D. Corneliussen, and N. H. Nachtrieb, J. Chem. Phys. 32, 447 (1960).
[61]R. A. Johnson, in *Diffusion in Body-Centered Cubic Metals* (American Society for Metals, Metals Park, Ohio, 1965), p. 357; Phys. Rev. 134, A1329 (1964).
[62]J. Crank, *The Mathematics of Diffusion* (Oxford U. P., London, 1956), p. 13.
[63]G. Martin, D. A. Blackburn, and Y. Adda, Phys. Status Solidi 23, 223 (1967).

PHYSICAL REVIEW B VOLUME 3, NUMBER 12 15 JUNE 1971

Helmholtz Free Energy of an Anharmonic Crystal to $O(\lambda^4)$*

R. C. Shukla
Physics Department, Brock University, St. Catharines, Ontario, Canada
and
E. R. Cowley
Physics Department, McMaster University, Hamilton, Ontario, Canada
(Received 10 February 1970)

All of the diagrams contributing to the Helmholtz free energy to $O(\lambda^4)$, for a crystal in which every atom is on a site of inversion symmetry, have been evaluated. The expressions given are valid for finite temperatures, and separate expressions are given for all cases where the double occurrence of phonon lines is important. Numerical calculations have been carried out for all the diagrams for a nearest-neighbor central-force model of a face-centered-cubic lattice in the high-temperature limit and in the leading-term approximation. Two separate techniques, a scanning method and the plane-wave expansion method, were used for the evaluation of each diagram. When applied to a Lennard-Jones potential it is found that none of the diagrams makes a negligibly small contribution and that the convergence of the perturbation expansion appears poor for $T > \frac{1}{3}T_m$.

I. INTRODUCTION

A knowledge of the anharmonic contributions to the Helmholtz free energy of a crystal is necessary for a complete understanding both of the properties of the solid itself and of the phenomenon of melting. Most approaches to this problem are based initially on the use of perturbation theory, but the systematic application of this technique is not well defined. The difficulty is that the use of perturbation theory leads to an anharmonic contribution to the free energy which is an infinite series in the perturbing potential, while the perturbation is itself an infinite series expansion of the cubic, quartic, and higher-order terms in the Taylor expansion of the potential energy of the crystal.

The traditional approach is to use an ordering scheme devised by Van Hove.[1] He introduced an ordering parameter, here called λ, equal in magnitude to a typical atomic displacement divided by the nearest-neighbor distance, and showed how the order of the various terms in the double series expansion could be obtained. The lowest-order anharmonic contributions to the free energy are then found to be of order λ^2. The derivation of these contributions, and their evaluation for a simple model, has been described by Maradudin, Flinn, and Coldwell-Horsfall.[2] The contribution to C_v from these diagrams is found to be proportional to T at high temperatures, but it has been found that this temperature dependence is inadequate to describe the experimental results for several

materials.[3] When terms beyond the lowest order are considered, the number of diagrams occurring increases rapidly, and, since the different diagrams have different structures, each must be evaluated separately.

An alternative approach is the self-consistent formalism of Choquard[4] and others. This is based on the summation of the infinite series of diagrams arising in a given order of perturbation theory, rather than the Van Hove ordering scheme. In the first-order self-consistent scheme (SC1), all first-order contributions to the phonon self-energies are summed, to give a set of renormalized frequencies, and then all ring diagrams containing first-order inserts are summed to give the free energy in the form of a harmonic free energy, but involving the renormalized frequencies. In the second-order self-consistent scheme (SC2) a similar procedure is carried through, except that all first- and second-order diagrams and inserts are summed. The self-consistency element in the theory is that the diagrams are to be evaluated with the renormalized frequencies. This leads to an iterative numerical procedure and also means that the theory is not simply perturbation theory.

Numerical calculations of SC1 theory have been made for the inert gas crystals by Goldman, Horton, and Klein.[5] As far as we are aware, no calculations have yet been made using SC2 theory, but Goldman *et al.* suggested an approximation intermediate between the first- and second-order theories. This is the improved self-consistent theory (ISC), which is the same as SC1, but supplemented by the most important second-order diagram evaluated using the renormalized frequencies and potential.

Each of these three approximations involves the selection of a subset of higher-order diagrams which are assumed to be the most important. In the present paper we derive all of the contributions of order λ^4, which is the next nonvanishing order, and evaluate them for the simple model used by Maradudin *et al.*

The derivation is described in Sec. II, and the numerical techniques and results are given in Sec. III. In Sec. IV we make a comparison of the contributions given by the subsets of diagrams included in the various approximate schemes. We conclude that while none of the approximations is successful in selecting the most important set of diagrams, the ISC scheme is most likely to give good agreement with experiment.

II. THEORY

The Hamiltonian of an anharmonic crystal to order λ^4 is given in second quantized form by

$$H = H_0 + H_A , \tag{1}$$

where

$$H_0 = \sum_{\lambda} \tfrac{1}{2}\hbar\omega(\lambda)\,[a(\lambda)\,a^*(\lambda) + a^*(\lambda)\,a(\lambda)]$$

and

$$H_A = \sum_{n=3}^{6} V(\lambda_1, \ldots, \lambda_n) A(\lambda_1) \cdots A(\lambda_n) .$$

Here λ_i stands for the double suffix $(\vec{q}_i j_i)$, $a^*(\lambda)$ and $a(\lambda)$ are the usual creation and destruction operators for the phonon λ, and

$$A(\lambda) = a(\lambda) + a^*(-\lambda) .$$

The coefficients $V(\lambda_1, \ldots, \lambda_n)$ are related to the coefficients $\Phi(\lambda_1, \ldots, \lambda_n)$ defined by Born and Huang[6] by

$$V(\lambda_1, \ldots, \lambda_n) = \left(\frac{1}{n!}\right) N^{1-n/2}\, \Delta(\vec{q}_1 + \cdots + \vec{q}_n) \times \left(\frac{\hbar^n}{2^n}\, \omega(\lambda_1) \cdots \omega(\lambda_n)\right)^{1/2} \Phi(\lambda_1, \ldots, \lambda_n).$$

The Helmholtz free energy (F) is given by

$$F = -k_B T \ln Z ,$$

where

$$Z = \mathrm{Tr}\, e^{-\beta H} , \quad \beta = 1/k_B T ,$$

and H is given by Eq. (1). As described in the review by Cowley,[7] it is possible to show that

$$F = F_0 - k_B T L ,$$

where F_0 is the Harmonic free energy and L is the contribution to the partition function from all connected diagrams.

In Van Hove's scheme, the order of a diagram is determined by counting a factor of λ^{n-2} for each n-phonon vertex. There are then three diagrams of order λ^2, shown in Fig. 1. Diagram 1(c) gives zero contribution for all Bravais lattices as well as for lattices with a basis provided that each atom is at a center of inversion symmetry. Diagrams 1(a) and 1(b) have been evaluated by several authors[2,7,8] and the contributions to F are

$$3 \sum_{\lambda_1 \lambda_2} V(-\lambda_1, \lambda_1, -\lambda_2, \lambda_2)\,[2n(\lambda_1) + 1]\,[2n(\lambda_2) + 1] \tag{2}$$

from Fig. 1(a) and

$$-\frac{6}{\hbar} \sum_{\lambda_1 \lambda_2 \lambda_3} |V(\lambda_1, \lambda_2, \lambda_3)|^2 f(\lambda_1, \lambda_2, \lambda_3), \tag{3a}$$

where

$$f(\lambda_1, \lambda_2, \lambda_3) = \frac{[n(\lambda_1) + 1]\,[n(\lambda_2) + n(\lambda_3) + 1] + n(\lambda_2) n(\lambda_3)}{\omega(\lambda_1) + \omega(\lambda_2) + \omega(\lambda_3)}$$

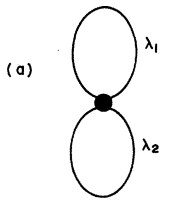

FIG. 1. Diagrams of order λ^2.

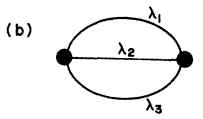

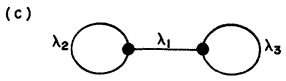

$$+3\,\frac{n(\lambda_1)n(\lambda_2)+n(\lambda_1)n(\lambda_3)-n(\lambda_2)n(\lambda_3)+n(\lambda_1)}{\omega(\lambda_2)+\omega(\lambda_3)-\omega(\lambda_1)} \tag{3b}$$

for diagram 1(b). $n(\lambda_i)$ are the Bose-Einstein population factors given by

$$n(\lambda_i)=(e^{\hbar\omega(\lambda_i)/k_BT}-1)^{-1}. \tag{4}$$

The diagrams of the next higher order, i.e., of order λ^4, are shown in Fig. 2. Diagrams similar in nature to diagram 1(c), which give zero contribution for every atom on a center of symmetry, have been omitted. The contributions from all of these diagrams can be evaluated following the rules given by Cowley.[7]

There is only one diagram of first order [Fig. 2(a)] and its contribution to F is

$$-\frac{1}{\beta}\,\frac{(-\beta)^1}{1!}\times 15\sum_{\lambda_1\lambda_2\lambda_3}\sum_{n_1n_2n_3}V(-\lambda_1,\lambda_1;-\lambda_2,\lambda_2;-\lambda_3,\lambda_3)$$
$$\times G(\lambda_1,i\omega_{n_1})G(\lambda_2,i\omega_{n_2})G(\lambda_3,i\omega_{n_3})\,. \tag{5}$$

The factor 15 comes from the number of pairing schemes. Substituting for the Fourier coefficient of the Green's function $G(\lambda,i\omega_n)$,

$$G(\lambda,i\omega_n)=\frac{2\omega(\lambda)}{\beta\hbar}\,\frac{1}{\omega_n^2+\omega(\lambda)^2}\,, \tag{6}$$

and performing the summations over n_1, n_2, and n_3 by Poisson's summation formula

$$\sum_n h(i\omega_n)=-\frac{\beta\hbar}{2\pi i}\int_c h(i\omega_n)f(i\omega_n)\,d(i\omega_n)\,, \tag{7}$$

where

$$f(i\omega_n)=(e^{(\beta\hbar i\omega_n)}-1)^{-1}\,, \tag{8}$$

we find for diagram 2(a)

$$15\sum_{\lambda_1\lambda_2\lambda_3}V(-\lambda_1,\lambda_1;-\lambda_2,\lambda_2;-\lambda_3,\lambda_3)$$
$$\times[2n(\lambda_1)+1][2n(\lambda_2)+1][2n(\lambda_3)+1]. \tag{9}$$

We note that any closed loop in a diagram leads to a factor of $[2n(\lambda)+1]$. There are three second-order diagrams [Figs. 2(b), 2(c), 2(e)]. The contribution from 2(b) is given by

$$-\frac{1}{\beta}\,\frac{(-\beta)^2}{2!}$$
$$\times 72\sum_{\lambda_1\lambda_2\lambda_3\lambda_4}V(-\lambda_1,\lambda_1,\lambda_2,\lambda_3)\,V(-\lambda_2,-\lambda_3,-\lambda_4,\lambda_4)$$
$$\times\sum_{n_1n_2n_3}G(\lambda_1,i\omega_{n_1})G(\lambda_3,i\omega_{n_3})G(\lambda_2,-i\omega_{n_3})G(\lambda_4,i\omega_{n_2})\,. \tag{10}$$

The factor 72 arises from the number of pairing schemes. Performing the summations we find

$$-\frac{72}{\hbar}\sum_{\lambda_1\lambda_2\lambda_3\lambda_4}V(-\lambda_1,\lambda_1,\lambda_2,\lambda_3)\,V(-\lambda_4,\lambda_4,-\lambda_2,-\lambda_3)$$
$$\times[2n(\lambda_1)+1]\,[2n(\lambda_4)+1]$$
$$\times\left\{\frac{1+n(\lambda_2)+n(\lambda_3)}{\omega(\lambda_2)+\omega(\lambda_3)}+\frac{n(\lambda_3)-n(\lambda_2)}{\omega(\lambda_2)-\omega(\lambda_3)}\right\} \tag{11}$$

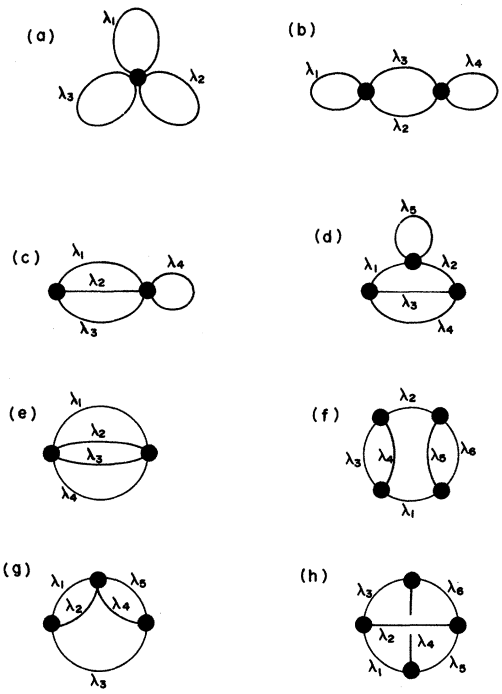

FIG. 2. Diagrams of order λ^4.

for the case $\lambda_2 \neq \lambda_3$. However, the phonons λ_2 and λ_3 are required by wave-vector conservation to correspond to the same wave vector, so that in the case of a Bravais lattice there is a one in three probability that $j_2 = j_3$.

It is therefore necessary to consider this case explicitly. The curly bracket then becomes

$$\{[\tfrac{1}{2} + n(\lambda_2)]/\omega(\lambda_2) + \beta\hbar n(\lambda_2)[1 + n(\lambda_2)]\} . \qquad (12)$$

Diagram 2(c) is similar in structure to diagram 1(b) and the summations over ω_n can be performed in exactly the same way to give

$$-\frac{120}{\hbar} \sum_{\lambda_1\lambda_2\lambda_3\lambda_4} V(\lambda_1, \lambda_2, \lambda_3)\, V(-\lambda_1, -\lambda_2, -\lambda_3, -\lambda_4, \lambda_4) \times [2n(\lambda_4) + 1]\, f(\lambda_1, \lambda_2, \lambda_3) , \qquad (13)$$

where $f(\lambda_1, \lambda_2, \lambda_3)$ is defined in Eq. 3(b) and the factor 120 corresponds to the product of the number of topologically equivalent diagrams (2 in the present case) and 60 pairing schemes.

The contribution of the last of the two-vertex diagrams [Fig. 2(e)] is given by

$$-\frac{1}{\beta}\frac{(-\beta)^2}{2!} \times 24 \sum_{\lambda_1\lambda_2\lambda_3\lambda_4} V(\lambda_1, \lambda_2, \lambda_3, \lambda_4)\, V(-\lambda_1, -\lambda_2, -\lambda_3, -\lambda_4) \times \sum_{n_1 n_2 n_3} G(\lambda_1, i\omega_{n_1}) G(\lambda_2, i\omega_{n_2}) G(\lambda_3, i\omega_{n_3})\, G(\lambda_4, -i\omega_{n_1} - i\omega_{n_2} - i\omega_{n_3}) . \qquad (14)$$

The factor 24 arises from the number of pairing schemes.

When Eq. (6) is substituted for the various propagators appearing in the above equation with different arguments and the product is resolved into partial fractions, a total of 16 terms have to be summed over n_1, n_2, and n_3. However, all of these terms can be written in the following general form:

$$\sum_{n_1 n_2 n_3} \frac{1}{(\omega_1 + ik_1\omega_{n_1})(\omega_2 + ik_2\omega_{n_2})(\omega_3 + ik_3\omega_{n_3})[\omega_4 + ik_4(\omega_{n_1} + \omega_{n_2} + \omega_{n_3})]} , \qquad (15)$$

where the 16 terms correspond to the various combinations of $k_i = \pm 1$, $i = 1, 2, 3, 4$. The summation over n_1, n_2, and n_3 can be performed as before and the final result for diagram 2(e) is

$$-\frac{12}{\hbar} \sum_{\lambda_1\lambda_2\lambda_3\lambda_4} |V(\lambda_1, \lambda_2, \lambda_3, \lambda_4)|^2 \sum_{k_1k_2k_3k_4} \frac{k_1k_2k_3k_4}{k_1\omega_1 + k_2\omega_2 + k_3\omega_3 - k_4\omega_4} \times \{N_1N_2N_4 + N_1N_4N_3 + N_2N_4N_3 - N_2N_1N_3 + N_4N_3 + N_2N_4 + N_1N_4 + N_4\} , \qquad (16)$$

where

$$N_i = \left[\exp\left(\frac{\hbar k_i \omega_i}{k_B T}\right) - 1\right]^{-1} , \quad N_i \equiv n_i \text{ for } k_i = +1, \text{ and } N_i \equiv -(n_i + 1) \text{ for } k_i = -1, \; i = 1, \ldots, n .$$

In this equation, and in similar equations later, k_1, k_2, etc., are to be summed over the values ± 1. The summations over k_1, k_2, k_3, k_4 can be performed and the terms rearranged to give

$$-\frac{12}{\hbar} \sum_{\lambda_1\lambda_2\lambda_3\lambda_4} |V(\lambda_1, \lambda_2, \lambda_3, \lambda_4)|^2 \left(\frac{(n_1+1)(n_2+1)(n_3+1)(n_4+1) - n_1n_2n_3n_4}{\omega_1 + \omega_2 + \omega_3 + \omega_4} + 4\,\frac{n_1(n_2+1)(n_3+1)(n_4+1) - (n_1+1)n_2n_3n_4}{\omega_2 + \omega_3 + \omega_4 - \omega_1} - 3\,\frac{n_1n_2(n_3+n_4+1) - n_3n_4(n_1+n_2+1)}{\omega_1 + \omega_2 - \omega_3 - \omega_4}\right) , \qquad (17)$$

where $n(\lambda_i) = n_i$, $\omega(\lambda_i) = \omega_i$, $i = 1, 2, 3 \ldots$.

The contributions from the two third-order diagrams [Figs. 2(d) and 2(g)] can be evaluated similarly. There are two types of contribution coming from diagram 2(d). The general expression is

$$-\frac{1}{\beta}\frac{(-\beta)^3}{3!} \times 3 \times 216 \sum_{\lambda_1\lambda_2\lambda_3\lambda_4\lambda_5} V(\lambda_1, \lambda_3, \lambda_4)\, V(-\lambda_5, \lambda_5, -\lambda_1, \lambda_2)\, V(-\lambda_2, -\lambda_3, -\lambda_4) \sum_{n_1n_2n_3} G(\lambda_1, i\omega_{n_1}) G(\lambda_2, i\omega_{n_1}) \times G(\lambda_5, i\omega_{n_3})\, G(\lambda_3, i\omega_{n_2}) G(\lambda_4, -i\omega_{n_1} - i\omega_{n_2}) . \qquad (18)$$

The factors 3 and 216 denote, respectively, the number of topologically equivalent diagrams and the number of pairing schemes. Substituting for the propagators and performing the summations exactly in the same manner as in diagram 2(e), for the case where all λ_1, λ_2, λ_3, λ_4, λ_5 are different, we find

$$+\frac{108}{(\hbar)^2}\sum_{\lambda_1\lambda_2\lambda_3\lambda_4\lambda_5} V(\lambda_1,\lambda_3,\lambda_4)\,V(-\lambda_5,\lambda_5,-\lambda_1,\lambda_2)\,V(-\lambda_2,-\lambda_3,-\lambda_4)\,[2n(\lambda_5)+1]$$

$$\times\left(\sum_{k_1k_2k_3k_4}\frac{k_1k_2k_3k_4}{k_2\omega_2-k_1\omega_1}\left\{\frac{N_1N_4-N_3N_1+N_3N_4+N_4}{k_1\omega_1+k_3\omega_3-k_4\omega_4}+\frac{N_2N_4-N_2N_3+N_3N_4+N_4}{k_4\omega_4-k_3\omega_3-k_2\omega_2}\right\}\right). \tag{19}$$

At this stage it is convenient to leave this expression in N notation, although one could write it in n notation as we have done before. There is a finite probability that $\lambda_1=\lambda_2$ in Fig. 2(d) and in this case $G(\lambda_1, i\omega_{n_1}) = G(\lambda_2, i\omega_{n_1})$. Performing the summations as before but now keeping in mind that there are poles of order 2, we find that the large parentheses in the previous expression are replaced by

$$\left(\sum_{k_1k_3k_4} k_3k_4\left\{\frac{(N_4-N_3)(N_1+1)+N_3(N_4+1)}{(k_1\omega_1+k_3\omega_3-k_4\omega_4)^2}+\beta\hbar\,\frac{N_1(N_1+1)(N_4-N_3)}{(k_1\omega_1+k_3\omega_3-k_4\omega_4)}\right\}\right.$$

$$\left.+2\sum_{k_3k_4}\frac{k_3k_4}{2\omega_1}\left\{\frac{(N_1+N_3+1)N_4-N_3N_1}{\omega_1+k_3\omega_3-k_4\omega_4}+\frac{(N_3-N_1)N_4+(N_1+1)N_3}{\omega_1-k_3\omega_3+k_4\omega_4}\right\}\right). \tag{20}$$

The contribution from the only remaining three-vertex diagram 2(g) is

$$-\frac{1}{\beta}\frac{(-\beta)^3}{3!}\times 3\times 216\sum_{\lambda_1\lambda_2\lambda_3\lambda_4\lambda_5} V(\lambda_1,\lambda_2,\lambda_3)\,V(-\lambda_1,-\lambda_2,\lambda_4,\lambda_5)\;V(-\lambda_3,-\lambda_4,-\lambda_5)$$

$$\times\sum_{n_1n_2n_3} G(\lambda_1,i\omega_{n_1})\,G(\lambda_2,i\omega_{n_2})\,G(\lambda_3,-i\omega_{n_1}-i\omega_{n_2})\,G(\lambda_4,i\omega_{n_3})\,G(\lambda_5,i\omega_{n_1}+i\omega_{n_2}-i\omega_{n_3}). \tag{21}$$

The factors 3 and 216 have the same origin as before in diagram 2(d). Performing the summations over n_1, n_2, n_3 we find

$$\frac{-108}{(\hbar)^2}\sum_{\lambda_1\lambda_2\lambda_3\lambda_4\lambda_5} V(\lambda_1,\lambda_2,\lambda_3)\,V(-\lambda_1,-\lambda_2,\lambda_4,\lambda_5)\,V(-\lambda_3,-\lambda_4,-\lambda_5)\sum_{k_1k_2k_3k_4k_5}\frac{k_1k_2k_3k_4k_5}{(k_1\omega_1+k_2\omega_2-k_3\omega_3)}$$

$$\times\left(\frac{(N_4N_5-N_3N_4-N_3N_5-N_3)(N_1+N_2+1)}{k_5\omega_5+k_4\omega_4-k_3\omega_3}+\frac{N_1N_2(N_4+N_5+1)-N_4N_5(N_1+N_2+1)}{k_5\omega_5+k_4\omega_4-k_2\omega_2-k_1\omega_1}\right). \tag{22}$$

Finally, we evaluate the contributions coming from the two four-vertex diagrams [Figs. 2(f) and 2(h)]. From diagram 2(f) there are two types of contribution. In general the contribution is

$$-\frac{1}{\beta}\frac{(-\beta)^4}{4!}\times 6\times 324\sum_{\lambda_1\lambda_2\lambda_3\lambda_4\lambda_5\lambda_6} V(\lambda_3,\lambda_4,\lambda_2)\,V(-\lambda_3,-\lambda_4,\lambda_1)\;V(-\lambda_1,\lambda_5,\lambda_6)\,V(-\lambda_5,-\lambda_6,-\lambda_2)$$

$$\times\sum_{n_1n_2n_3} G(\lambda_3,i\omega_{n_3})\;G(\lambda_4,i\omega_{n_1}-i\omega_{n_3})\,G(\lambda_1,i\omega_{n_1})\,G(\lambda_2,-i\omega_{n_1})\,G(\lambda_5,i\omega_{n_2})\,G(\lambda_6,i\omega_{n_1}-i\omega_{n_2}). \tag{23}$$

The factors 6 and 324 arise from the number of topologically equivalent diagrams and the number of pairing schemes, respectively. Now, for the case where λ_1 and λ_2 are different, we can perform the summations as before and the final result is

$$+\frac{81}{\hbar^3}\sum_{\lambda_1\lambda_2\lambda_3\lambda_4\lambda_5\lambda_6} V(\lambda_3,\lambda_4,\lambda_2)V(-\lambda_3,-\lambda_4,\lambda_1)V(-\lambda_1,\lambda_5,\lambda_6)\;V(-\lambda_5,-\lambda_6,-\lambda_2)$$

$$\times\left[\sum_{k_1k_2k_3k_4k_5k_6} k_1k_2k_3k_4k_5k_6\left\{(N_3+N_4+1)(N_5+N_6+1)\;\left(\frac{N_1+1}{D_1}+\frac{N_2+1}{D_2}\right)\right.\right.$$

$$+\frac{(N_3+1)(N_4+1)(N_5+N_6+1)}{D_3}+\frac{(N_5+1)(N_6+1)(N_3+N_4+1)}{D_4}\Bigg\}\Bigg], \tag{24}$$

where

$$D_1=(k_1\omega_1-k_2\omega_2)(k_4\omega_4-k_1\omega_1+k_3\omega_3)(k_6\omega_6-k_1\omega_1+k_5\omega_5),$$

$$D_2=(k_2\omega_2-k_1\omega_1)(k_4\omega_4-k_2\omega_2+k_3\omega_3)(k_6\omega_6-k_2\omega_2+k_5\omega_5),$$

$$D_3=(k_4\omega_4+k_3\omega_3-k_1\omega_1)(k_2\omega_2-k_3\omega_3-k_4\omega_4)(k_6\omega_6-k_4\omega_4+k_5\omega_5-k_3\omega_3),$$

$$D_4=(k_6\omega_6+k_5\omega_5-k_1\omega_1)(k_2\omega_2-k_5\omega_5-k_6\omega_6)(k_3\omega_3+k_4\omega_4-k_5\omega_5-k_6\omega_6),$$

when $\lambda_1=\lambda_2$, the quantity inside the square brackets in the previous expression [Eq. (24)] is to be replaced by

$$\sum_{k_1k_3k_4k_5k_6}k_3k_4k_5k_6\Bigg\{\frac{1}{k_6\omega_6+k_5\omega_5-k_4\omega_4-k_3\omega_3}\left(\frac{(N_3+N_4+1)(N_5+1)(N_6+1)}{(k_1\omega_1-k_5\omega_5-k_6\omega_6)^2}-\frac{(N_3+1)(N_4+1)(N_5+N_6+1)}{(k_1\omega_1-k_3\omega_3-k_4\omega_4)^2}\right)$$

$$+\frac{(N_1+1)(N_3+N_4+1)(N_5+N_6+1)}{(k_3\omega_3+k_4\omega_4-k_1\omega_1)(k_5\omega_5+k_6\omega_6-k_1\omega_1)}\left(\frac{1}{(k_3\omega_3+k_4\omega_4-k_1\omega_1)}+\frac{1}{(k_5\omega_5+k_6\omega_6-k_1\omega_1)}-\beta\hbar N_1\right)\Bigg\}$$

$$+2\sum_{k_3k_4k_5k_6}(-k_3k_4k_5k_6)\Bigg\{\frac{(N_3+N_4+1)(N_5+N_6+1)}{2\omega_1}$$

$$\times\left(\frac{n_1+1}{(k_6\omega_6+k_5\omega_5-\omega_1)(k_4\omega_4+k_3\omega_3-\omega_1)}+\frac{n_1}{(k_4\omega_4+k_3\omega_3+\omega_1)(k_6\omega_6+k_5\omega_5+\omega_1)}\right)$$

$$-\frac{(N_3+1)(N_4+1)(N_5+N_6+1)}{(k_4\omega_4+k_3\omega_3+\omega_1)(k_4\omega_4+k_3\omega_3-\omega_1)(k_6\omega_6+k_5\omega_5-k_4\omega_4-k_3\omega_3)}$$

$$-\frac{(N_5+1)(N_6+1)(N_3+N_4+1)}{(k_6\omega_6+k_5\omega_5+\omega_1)(k_6\omega_6+k_5\omega_5-\omega_1)(k_3\omega_3+k_4\omega_4-k_5\omega_5-k_6\omega_6)}\Bigg\}. \tag{25}$$

The contribution from the remaining four-vertex diagram, one of the most complicated ones encountered so far, is

$$-\frac{1}{\beta}\frac{(-\beta)^4}{4!}\times1\times1296\sum_{\lambda_1,\lambda_2,\lambda_3,\lambda_4,\lambda_5,\lambda_6}V(\lambda_1,\lambda_2,\lambda_3)V(-\lambda_1,\lambda_4,\lambda_5)V(-\lambda_2,-\lambda_5,\lambda_6)\ V(-\lambda_3,-\lambda_4,-\lambda_6)$$

$$\times\sum_{n_1n_2n_3}G(\lambda_1,i\omega_{n_1})G(\lambda_2,i\omega_{n_2})G(\lambda_3,-i\omega_{n_1}-i\omega_{n_2})\ G(\lambda_4,i\omega_{n_3})G(\lambda_5,i\omega_{n_1}-i\omega_{n_3})G(\lambda_6,i\omega_{n_2}+i\omega_{n_3}). \tag{26}$$

The factor 1296 equals the number of different pairing schemes corresponding to one topologically equivalent diagram. Substituting for G's from Eq. (3), the general term can be easily written down. Performing the summations over n_1, n_2, n_3, the final result is

$$\frac{54}{(\hbar)^3}\sum_{\lambda_1,\lambda_2,\lambda_3,\lambda_4,\lambda_5,\lambda_6}V(\lambda_1,\lambda_2,\lambda_3)V(-\lambda_1,\lambda_4,\lambda_5)V(-\lambda_2,-\lambda_5,\lambda_6)$$

$$\times V(-\lambda_3,-\lambda_4,-\lambda_6)\sum_{k_1,k_2,k_3,k_4,k_5,k_6}k_1k_2k_3k_4k_5k_6H(k_1,k_2,k_3,k_4,k_5,k_6), \tag{27}$$

where

$$H(k_1,\ldots,k_6)=H_1+H_2+H_3+H_4+H_5+H_6\ ,$$

$$H_1 = \frac{(N_6 - N_2)[(N_1 - N_5)(N_4 + 1) + N_5(N_1 + 1)]}{(k_3\omega_3 - k_2\omega_2 - k_1\omega_1)(k_6\omega_6 - k_4\omega_4 - k_2\omega_2)(k_5\omega_5 + k_4\omega_4 - k_1\omega_1)} ,$$

$$H_2 = \frac{(N_4 - N_1)[(N_3 - N_5)(N_6 + 1) + N_5(N_3 + 1)]}{(k_1\omega_1 + k_2\omega_2 - k_3\omega_3)(k_6\omega_6 + k_5\omega_5 - k_3\omega_3)(k_5\omega_5 + k_4\omega_4 - k_1\omega_1)} ,$$

$$H_3 = \frac{N_2(N_5 + 1)(N_6 + 1) + N_5(N_1 + 1)(N_6 + 1) - N_2(N_1 + 1)(N_6 + 1) - N_5(N_1 + 1)(N_2 + 1)}{(k_1\omega_1 + k_2\omega_2 - k_3\omega_3)(k_6\omega_6 - k_4\omega_4 - k_2\omega_2)(k_6\omega_6 + k_5\omega_5 - k_2\omega_2 - k_1\omega_1)} ,$$

$$H_4 = \frac{(N_3 - N_5)[(N_6 - N_2)(N_4 + 1) + N_2(N_6 + 1)]}{(k_1\omega_1 + k_2\omega_2 - k_3\omega_3)(k_6\omega_6 - k_4\omega_4 - k_2\omega_2)(k_6\omega_6 + k_5\omega_5 - k_3\omega_3)} , \qquad (28)$$

$$H_5 = \frac{N_3(N_1 + 1)(N_6 + 1) - N_1(N_3 + 1)(N_4 + 1) + (N_1 + 1)(N_4 + 1)(N_6 + 1) - (N_3 + 1)(N_4 + 1)(N_6 + 1)}{(k_1\omega_1 + k_2\omega_2 - k_3\omega_3)(k_5\omega_5 + k_4\omega_4 - k_1\omega_1)(k_6\omega_6 - k_4\omega_4 - k_3\omega_3 + k_1\omega_1)} ,$$

$$H_6 = \frac{(N_2 + 1)(N_4 + 1)(N_5 + 1) - N_5(N_3 + 1)(N_4 + 1) - (N_2 + 1)(N_3 + 1)(N_4 + 1) - N_2N_5(N_3 + 1)}{(k_1\omega_1 + k_2\omega_2 - k_3\omega_3)(k_6\omega_6 + k_5\omega_5 - k_3\omega_3)(k_5\omega_5 + k_4\omega_4 - k_3\omega_3 + k_2\omega_2)} .$$

In the high-temperature limit, the expressions contributing to F from all the diagrams discussed in this section, viz., 1(a), 1(b), and 2(a)–2(h), have been presented in Table I.

Finally, if there are n lines joining two vertices, the contribution to F has been evaluated and presented in the Appendix.

III. NUMERICAL RESULTS

We have evaluated each of the contributions described in Sec. II, in the high-temperature limit, for a model of a face-centered-cubic crystal with a nearest-neighbor central interaction in the leading-term approximation. In this approximation, the tensor derivatives of the two-body potential at the point (x, y, z), at distance r, are approximated by

TABLE I. High-temperature limits for the various contributions to the free energy.

Diagram	High-temperature limit
1(a)	$\frac{3}{\beta^2}\left(\frac{2}{\hbar}\right)^2 \sum_{\lambda_1,\lambda_2} \frac{V(\lambda_1, -\lambda_1, \lambda_2, -\lambda_2)}{\omega(\lambda_1)\omega(\lambda_2)}$
1(b)	$-\frac{3}{\beta^2}\left(\frac{2}{\hbar}\right)^3 \sum_{\lambda_1,\lambda_2,\lambda_3} \frac{\lvert V(\lambda_1, \lambda_2, \lambda_3)\rvert^2}{\omega(\lambda_1)\omega(\lambda_2)\omega(\lambda_3)}$
2(a)	$\frac{15}{\beta^3}\left(\frac{2}{\hbar}\right)^3 \sum_{\lambda_1,\lambda_2,\lambda_3} \frac{V(\lambda_1, -\lambda_1, \lambda_2, -\lambda_2, \lambda_3, -\lambda_3)}{\omega(\lambda_1)\omega(\lambda_2)\omega(\lambda_3)}$
2(b)	$-\frac{36}{\beta^3}\left(\frac{2}{\hbar}\right)^4 \sum_{\lambda_1,\lambda_2,\lambda_3,\lambda_4} \frac{V(\lambda_1, -\lambda_1, \lambda_2, \lambda_3)V(-\lambda_2, -\lambda_3, \lambda_4, -\lambda_4)}{\omega(\lambda_1)\omega(\lambda_2)\omega(\lambda_3)\omega(\lambda_4)}$
2(c)	$-\frac{60}{\beta^3}\left(\frac{2}{\hbar}\right)^4 \sum_{\lambda_1,\lambda_2,\lambda_3,\lambda_4} \frac{V(\lambda_1, \lambda_2, \lambda_3)V(-\lambda_1, -\lambda_2, -\lambda_3, \lambda_4, -\lambda_4)}{\omega(\lambda_1)\omega(\lambda_2)\omega(\lambda_3)\omega(\lambda_4)}$
2(d)	$\frac{108}{\beta^3}\left(\frac{2}{\hbar}\right)^5 \sum_{\lambda_1,\lambda_2,\lambda_3,\lambda_4,\lambda_5} \frac{V(\lambda_1, \lambda_3, \lambda_4)V(-\lambda_2, -\lambda_3, -\lambda_4)V(-\lambda_1, \lambda_2, \lambda_5, -\lambda_5)}{\omega(\lambda_1)\omega(\lambda_2)\omega(\lambda_3)\omega(\lambda_4)\omega(\lambda_5)}$
2(e)	$-\frac{12}{\beta^3}\left(\frac{2}{\hbar}\right)^4 \sum_{\lambda_1,\lambda_2,\lambda_3,\lambda_4} \frac{\lvert V(\lambda_1, \lambda_2, \lambda_3, \lambda_4)\rvert^2}{\omega(\lambda_1)\omega(\lambda_2)\omega(\lambda_3)\omega(\lambda_4)}$
2(f)	$-\frac{81}{\beta^3}\left(\frac{2}{\hbar}\right)^6 \sum_{\lambda_1,\lambda_2,\lambda_3,\lambda_4,\lambda_5,\lambda_6} \frac{V(\lambda_1, \lambda_3, \lambda_4)V(-\lambda_1, \lambda_5, \lambda_6)V(\lambda_2, -\lambda_3, -\lambda_4)V(-\lambda_2, -\lambda_5, -\lambda_6)}{\omega(\lambda_1)\omega(\lambda_2)\omega(\lambda_3)\omega(\lambda_4)\omega(\lambda_5)\omega(\lambda_6)}$
2(g)	$\frac{108}{\beta^3}\left(\frac{2}{\hbar}\right)^5 \sum_{\lambda_1,\lambda_2,\lambda_3,\lambda_4,\lambda_5} \frac{V(\lambda_1, \lambda_2, \lambda_4, \lambda_5)V(-\lambda_1, -\lambda_2, \lambda_3)V(-\lambda_3, -\lambda_4, -\lambda_5)}{\omega(\lambda_1)\omega(\lambda_2)\omega(\lambda_3)\omega(\lambda_4)\omega(\lambda_5)}$
2(h)	$-\frac{54}{\beta^3}\left(\frac{2}{\hbar}\right)^6 \sum_{\lambda_1,\lambda_2,\lambda_3,\lambda_4,\lambda_5,\lambda_6} \frac{V(\lambda_1, \lambda_2, \lambda_3)V(-\lambda_1, \lambda_4, \lambda_5)V(-\lambda_2, -\lambda_5, \lambda_6)V(-\lambda_3, -\lambda_4, -\lambda_6)}{\omega(\lambda_1)\omega(\lambda_2)\omega(\lambda_3)\omega(\lambda_4)\omega(\lambda_5)\omega(\lambda_6)}$

$$\frac{\partial^n \phi}{\partial x\, \partial y \cdots \partial z} \simeq \frac{xy\cdots z}{r^n}\ \phi^n\ , \tag{29}$$

where ϕ^n is the nth derivative of the potential ϕ with respect to the scalar distance r, evaluated at the nearest neighbor r_0. Leech and Reissland[9] have recently given an example of the size of error which this approximation can cause, about 30% in their case. However, the simplifications in the numerical procedures which result from the approximation are considerable, so that it seems reasonable to make it in a first evaluation of the higher-order diagrams.

The most important merit of the model is that certain sums can be carried out analytically. In particular, Maradudin *et al.*[2] have shown that, if $(l_\alpha, l_\beta, l_\gamma)$ is a vector separating an atom from one of its nearest neighbors,

$$\sum_{\alpha\beta}\sum_{\vec{q}j} \frac{e_\alpha(\vec{q}j)\, e_\beta(\vec{q}j) l_\alpha l_\beta}{l^2\omega^2(\vec{q}j)} [1-\cos(\vec{q}\cdot\vec{l})] = \frac{NM}{4\phi''}\ . \tag{30}$$

The sum over $\vec{q}j$ is over the $3N$ independent normal modes of the crystal, with eigenvector $\vec{e}(\vec{q}j)$ and frequencies $\omega(\vec{q}j)$. N is the number of unit cells and m is the atomic mass. This expression appears in the contribution from any diagram containing closed loops, and the use of the above relation allows all such loops to be evaluated. A second useful relation is

$$\sum_{\alpha\beta}\sum_{\vec{l}} \frac{l_\alpha l_\beta e_\alpha(\vec{q}j_1)\, e_\beta(\vec{q}j_2)}{\omega(\vec{q}j_1)\omega(\vec{q}j_2) l^2}\ [1-\cos(\vec{q}\cdot\vec{l})] = \frac{M}{\phi''}\ \delta_{j_1,j_2}\ . \tag{31}$$

The second sum is over the twelve nearest-neighbor positions.

A number of diagrams cannot be evaluated analytically. For these we use the plane-wave expansion to eliminate the δ functions, which express wave-vector conservation at each vertex. That is, we write

$$N\Delta(\vec{q}_1+\cdots+\vec{q}_i) = \sum_{\vec{n}} \exp[i\vec{n}\cdot(\vec{q}_1+\cdots+\vec{q}_i)]\ . \tag{32}$$

The sum is over all vectors of the real lattice, but the expressions which result when this substitution is made in the free-energy contribution converge sufficiently rapidly with $\vec{n}$ for the technique to be useful. All of the sums over the Brillouin zone which remain can be put in the form

$$\sum_{\vec{q}j} \frac{e_\alpha(\vec{q}j)\, e_\beta(\vec{q}j)}{\omega^2(\vec{q}j)} \cos(\vec{q}\cdot\vec{n})\ . \tag{33}$$

Our procedure was to tabulate these sums for a large number of values of the vector $\vec{n}$. The Brillouin-zone summations were then done once only, with a mesh of points corresponding to 1372 wave vectors in the whole zone. The contribution from the wave vector (0, 0, 0) was omitted and the sums were normalized by a factor of 1371.

A second method of calculation is to perform each of the sums over the normal modes for a finite mesh of wave vectors distributed uniformly through the Brillouin zone. The calculation is then straightforward, the only subtle feature being the normalization of the sums. This has been discussed for diagram 1(b) by Klein, Goldman, and Horton,[10] and similar precautions can be taken for all of the diagrams. We have evaluated each of the diagrams requiring numerical calculation by both techniques. In the results which follow the method which seemed most appropriate is indicated for each diagram separately.

Using the techniques outlined above, Maradudin *et al.*[2] evaluated the two diagrams (a) and (b) of Fig. 1, in the high-temperature limit, to give

$$\text{for 1(a):}\quad 0.1875N(k_BT)^2\phi^{iv}/[\phi'']^2\ , \tag{34}$$

$$\text{for 1(b):}\quad -0.05609N(k_BT)^2[\phi'''']^2/[\phi'']^3\ . \tag{35}$$

The numerical coefficient in 1(a) is exact.

Using the same techniques the diagrams (a) and (b) of Fig. 2 can be evaluated analytically to give

$$\text{for 2(a):}\quad 0.015625N(k_BT)^3\phi^{vi}/[\phi'']^3\ , \tag{36}$$

$$\text{for 2(b):}\quad -0.046875N(k_BT)^3[\phi^{iv}]^2/[\phi'']^4\ . \tag{37}$$

Diagrams 2(c) and 2(d) can be related analytically to diagram (b) of Fig. 1, and using the previously quoted result we get

$$\text{for 2(c):}\quad -0.02805N(k_BT)^3\phi'''\phi^{v}/[\phi'']^4\ , \tag{38}$$

$$\text{for 2(d):}\quad 0.04207N(k_BT)^3[\phi''']^2\phi^{iv}/[\phi'']^5\ . \tag{39}$$

Diagram 2(e) can be evaluated by almost exactly the same technique as described by Maradudin *et al.* for diagram (b) of Fig. 1, to give

$$\text{for 2(e):}\quad -0.00813N(k_BT)^3[\phi^{iv}]^2/[\phi'']^4\ . \tag{40}$$

The coefficient was calculated by the plane-wave method, values of n out to (3, 2, 1) were considered, but the contributions from vectors larger than (2, 2, 0) were negligible. The direct summation method gave the same answer to within $\frac{1}{2}\%$, with a mesh of 107 finite wave vectors in the whole zone, but required considerably longer computing time.

The plane-wave method is much less suitable for diagram (f), the reason being that there are three independent values of the vectors $\vec{n}$ to be summed over, as opposed to one independent value for diagrams 1(b) and 2(e). On the other hand, the direct summation method is well suited and with a mesh of 499 finite wave vectors we obtained

for 2(f): $-0.00956N(k_BT)^3[\phi'''']^4/[\phi'']^6$. (41)

The best value obtained with the plane-wave method was within 20% of this, and the sums were clearly not fully converged.

For diagram 2(g) we obtain the result

$$0.0196N(k_BT)^3\phi^{iv}[\phi'''']^2/[\phi'']^5. \quad (42)$$

The coefficient is an average of the values obtained using the two methods, the two separate answers agreeing to 1%. For the direct summation a mesh of 499 finite wave vectors was used, and in the plane-wave method seven independent pairs of $\vec{n}$'s, equivalent by symmetry to a total of 1621 pairs, were included in the summation. Neither method is clearly superior for this diagram.

Diagram 2(h) is time consuming whichever method is used. In the direct summation method the sums over the phonons are nested very deeply, and we were able to use only a mesh of 63 finite wave vectors. In the plane-wave method there are again three independent $\vec{n}$'s to be summed, and the convergence was very slow, as for diagram 2(f). The final result we obtain is

for 2(h): $-0.0023N(k_BT)^3[\phi'''']^4/[\phi'']^6$, (43)

and we estimate the uncertainty in the coefficient to be ± 0.0005. Fortunately this is the smallest contribution, so that this large percentage uncertainty is not important.

IV. DISCUSSION

In order to make a direct comparison of the magnitude of the various contributions evaluated in Sec. III, it is necessary to assume some form for the two-body potential. We assume here a 12-6 form

$$\phi = \epsilon[(r_0/r)^{12} - 2(r_0/r)^6] \quad (44)$$

and assume further that the separation r_0, corresponding to the minimum of ϕ, is the nearest-neighbor separation in the crystal. The ratios of derivatives which occur in the different contributions to the free energy can then each be written as a dimensionless number divided by ϵ^2, and the contributions to the free energy of order λ^4, in the high-temperature limit, contain a common factor of $N(k_BT)^3/\epsilon^2$. The contributions in these units are listed in Table II. The first column gives the label of the diagram in Fig. 2, and the second column gives the contribution to the free energy arising from the diagram. The numbers in the third column are the sums of the first two contributions, of the first four, of the first six, and of all the diagrams, respectively. They are grouped in this way because, of the diagrams we have considered, the first two are included in the set summed in the SC1 theory, the first four are included in ISC, and the first six in SC2. In particular, diagrams 2(c) and 2(d) represent the effect of using the smeared potential and the self-consistent basis functions in the evaluation of diagram 1(b).

TABLE II. Contributions to the free energy of $O(\lambda^4)$, for the 12-6 potential, in units of $N(k_BT)^3/\epsilon^2$.

Diagram	Contribution	Partial total
2(a)	0.345	$F(\mathrm{SC1}) = -0.899$
2(b)	−1.244	
2(c)	−0.732	
2(d)	1.328	$F(\mathrm{ISC}) = -0.303$
2(e)	−0.216	
2(f)	−0.359	$F(\mathrm{SC2}) = -0.878$
2(g)	0.619	
2(h)	−0.086	$F(\lambda^4) = -0.345$

Diagrams 2(g) and 2(h) are not included in any of the approximate schemes. Thus, the numbers in the third column of Table II give some indication of the relative merits of the various approximate schemes in selecting the most important diagrams of this order. Because of the iterative feature of the self-consistent schemes, the comparison is not exact.

It is clear that none of the approximations is really successful, and that the Van Hove ordering scheme is in fact very good. As predicted by Choquard,[4] the more highly connected diagrams give the smallest contributions. This can be seen, for example, in the series of diagrams 2(b), 2(c), and 2(e). The most highly connected diagram, 2(h), makes the smallest contribution, but even it is equal to a quarter of the total. Of the three partial sums, only ISC gives a subtotal which is close to the complete value, but this is due to the large cancellation which occurs between the neglected diagrams rather than because these diagrams individually give small contributions.

One qualification must be made to the above conclusions. We have evaluated each of the diagrams using the harmonic phonons as basis functions, whereas in the various self-consistent schemes, the basis functions are the self-consistent phonons. This can alter the magnitudes of the neglected contributions and, hopefully, reduce them. As an example of this, consider diagram 1(b). This is the most important diagram neglected in the SC1 theory, and it gives a negative contribution to the free energy. Diagrams 2(c) and 2(d) together give the lowest-order change in the value of this diagram when it is evaluated using the self-consistent basis functions, and from Table II it can be seen that the over-all effect is to reduce the contribution from the diagram. There seems to be no rigorous argument to show that the use of the self-consistent

basis functions always leads to smaller values for the neglected contributions, but such may often be the case, and the self-consistent approximations are probably better than the comparison made here suggests.

As far as the convergence of the perturbation expansion is considered, in the high-temperature limit the ratio of the total contribution of order λ^4 to that of order λ^2 is

$$F(\lambda^4)/F(\lambda^2) = -0.554(k_B T/\epsilon) \tag{45}$$

for the model we have used. For the inert-gas crystals, the potential well depth ϵ corresponds to a temperature of approximately twice the melting temperature. The convergence of the perturbation expansion is, then, in our opinion, just sufficiently good for the expansion to be useful. However, this estimate could be changed if, for example, the leading-term approximation was not made. The difficulty, a common one in calculations of anharmonic properties, is that the cancellation between the various diagrams is strong.

It is found that none of the diagrams can be ignored, although the subset of diagrams included in ISC theory gives a result close to the final total because of cancellations in the remaining terms.

The lowest-order approximation is then inadequate for temperatures greater than about one-third of the melting temperature, in agreement with the conclusions of Klein *et al.*[11]

ACKNOWLEDGMENTS

We would like to thank Tim Lahey for performing some calculations and Mrs. J. Cowan for typing the manuscript.

APPENDIX

The general sum for diagram 1(b), in the notation explained in Sec. II along with $z_\alpha = i\omega_{n_\alpha}$, $\alpha = 1, 2, \ldots, n$, is

$$\sum_{k_1,k_2,k_3} \sum_{n_1,n_2} \frac{1}{(\omega_1 + k_1 z_1)(\omega_2 + k_2 z_2)(\omega_3 + k_3 z_1 + k_3 z_2)} . \tag{A1}$$

Performing the summations over n_1 and n_2, this is equal to

$$\sum_{k_1,k_2,k_3} (-1)^2 k_1 k_2 k_3 \frac{[N(-\omega_1/k_1) - N(-\omega_3/k_3)][N(-\omega_2/k_2) - N(\omega_1/k_1 - \omega_3/k_3)]}{k_3\omega_3 - k_1\omega_1 - k_2\omega_2} . \tag{A2}$$

When the summations over k_1, k_2, k_3 are carried out, this yields the same equation as Eq. (3) in Sec. II. Similarly, for diagram 2(e) the general sum is

$$\sum_{k_1,k_2,k_3,k_4} \sum_{n_1,n_2,n_3} \frac{1}{(\omega_1 + k_1 z_1)(\omega_2 + k_2 z_2)(\omega_3 + k_3 z_3)(\omega_4 + k_4 z_1 + k_4 z_2 + k_4 z_3)} \tag{A3}$$

which is equal to

$$\sum_{k_1,k_2,k_3,k_4} (-1)^3 k_1 k_2 k_3 k_4$$

$$\times \frac{[N(-\omega_1/k_1) - N(-\omega_4/k_4)][N(-\omega_2/k_2) - N(\omega_1/k_1 - \omega_4/k_4)][N(-\omega_3/k_3) - N(\omega_1/k_1 + \omega_2/k_2 - \omega_4/k_4)]}{k_4\omega_4 - k_1\omega_1 - k_2\omega_2 - k_3\omega_3} \tag{A4}$$

after performing the summations over n_1, n_2, and n_3.

If there are n lines connecting the two vertices, the diagram would be similar to Fig. 2(e) and the general sum will be given by

$$\sum_{k_1,\ldots,k_n} \sum_{n_1,\ldots,n_{n-1}} \left[1 \Big/ \prod_{i=1}^{n-1} (\omega_i + k_i z_i) \left(\omega_n + k_n \sum_{j=1}^{n-1} z_j \right) \right] . \tag{A5}$$

Performing the summations over $n_1, \ldots, n_{n-1}$, this is equal to

$$\sum_{k_1,\ldots,k_n} (-1)^n \prod_{i=1}^{n} k_i \left[N\left(-\frac{\omega_1}{k_1}\right) - N\left(-\frac{\omega_n}{k_n}\right) \right]$$

$$\times \frac{[N(-\omega_2/k_2) - N(\omega_1/k_1 - \omega_n/k_n)] \cdots \{N(-\omega_{n-1}/k_{n-1}) - N[\sum_{l=1}^{n-2} (\omega_l/k_l - \omega_n/k_n)]\}}{k_n\omega_n - k_{n-1}\omega_{n-1} \cdots k_1\omega_1}, \tag{A6}$$

and the contribution to the Helmholtz free energy is equal to

$$-\frac{1}{\beta}\frac{(-\beta)^2}{2!}\, n! \sum_{\lambda_1 \cdots \lambda_n} |V(\lambda_1, \lambda_2, \ldots, \lambda_n)|^2$$

$$\times \sum_{n_1, n_2, \ldots, n_{n-1}} G(\lambda_1, i\omega_{n_1}) G(\lambda_2, i\omega_{n_2}) \cdots G(\lambda_{n-1}, i\omega_{n-1}) G(\lambda_n, -i\omega_{n_1} - i\omega_{n_2} \cdots - i\omega_{n_{n-1}})$$

$$= -\frac{1}{\hbar}\frac{n!}{2!} \sum_{\lambda_1 \cdots \lambda_n} |V(\lambda_1, \lambda_2, \ldots, \lambda_n)|^2 \times \text{Eq. (A6)}. \tag{A7}$$

*Work supported by the National Research Council of Canada.

[1]L. Van Hove, *Quantum Theory of Many Particle Systems* (Benjamin, New York, 1961).

[2]A. A. Maradudin, P. A. Flinn, and R. A. Coldwell-Horsfall, Ann. Phys. (N. Y.) 15, 360 (1961).

[3]C. R. Brooks, J. Phys. Chem. Solids 29, 1377 (1968); A. J. Leadbetter, D. M. T. Newsham, and G. R. Settatree, J. Phys. C 2, 393 (1969).

[4]P. F. Choquard, *The Anharmonic Crystal* (Benjamin, New York, 1967).

[5]V. V. Goldman, G. K. Horton, and M. L. Klein, Phys. Rev. Letters 21, 1527 (1968).

[6]M. Born and K. Huang, *The Dynamical Theory of Crystal Lattices* (Clarendon, Oxford, England, 1954).

[7]R. A. Cowley, Advan. Phys. 12, 421 (1963).

[8]W. Ludwig, J. Phys. Chem. Solids 4, 283 (1958).

[9]J. W. Leech and J. A. Reissland, J. Phys. C 3, 975 (1970); 3, 987 (1970).

[10]M. L. Klein, V. V. Goldman, and G. K. Horton, J. Phys. C 2, 1542 (1969).

[11]M. L. Klein, G. K. Horton, and J. L. Feldman, Phys. Rev. 184, 968 (1969).

PHYSICAL REVIEW B VOLUME 3, NUMBER 12 15 JUNE 1971

Superconductivity and Lattice Dynamics of White Tin

J. M. Rowell, W. L. McMillan, and W. L. Feldmann
Bell Telephone Laboratories, Murray Hill, New Jersey 07974

(Received 6 January 1971)

We present the results of a tunneling investigation and the details of the electron-phonon interaction in superconducting tin. From an iterative solution of the Eliashberg gap equations, the phonon spectrum, weighted by the square of the electron-phonon coupling constant, is determined. Comparison of this result with neutron scattering data suggests that, as in Pb, off-symmetry directions must be considered carefully in any determination of the tin phonon spectrum. The resolution and reproducibility of the tunneling technique is discussed at some length; in particular, we show that the Coulomb pseudopotential μ^* is extremely sensitive to small experimental errors. We suggest that a value of μ^* near the theoretical value of 0.10 can be taken as an indication of acceptably accurate experimental measurements.

I. INTRODUCTION

During the past six years a new technique for the study of both superconductivity and lattice dynamics has been developed. This technique, using electron tunneling into a superconductor, allows us to probe the details of the electron-phonon interaction that determines the superconductivity of the material. In this paper we present the results of such an investigation of the properties of white tin. The phonon spectrum, weighted by the square of the electron-phonon coupling constant, is determined. Comparison of this result with neutron scattering data suggests that, as in Pb, off-symmetry directions must be considered carefully in any determination of the tin phonon spectrum.

The first measurement of a superconducting property using the tunneling technique was made by Giaever[1] when he demonstrated the existence of the energy gap and, above the energy gap, the